frontiers | Frontiers in Materials

TYPE Original Research
PUBLISHED 09 December 2022
DOI 10.3389/fmats.2022.1071316

OPEN ACCESS

EDITED BY
Dong Zhang,
Fuzhou University, China

REVIEWED BY
Meng Guo,
Beijing University of Technology, China
Peiwen Hao,
Chang'an University, China
Yiwei Weng,
Hong Kong Polytechnic University,
Hong Kong SAR, China

*CORRESPONDENCE
Zuo-Cai Wang,
wangzuocai@hfut.edu.cn

SPECIALTY SECTION
This article was submitted to Structural Materials, a section of the journal Frontiers in Materials

RECEIVED 16 October 2022
ACCEPTED 28 November 2022
PUBLISHED 09 December 2022

CITATION
Niu S-L, Wang J-Y, Wang Z-C, Wang D-H, Sun X-T and Zhao X (2022), Overall feasibility assessment of polyester polyurethane concrete used as steel bridge deck pavement. *Front. Mater.* 9:1071316. doi: 10.3389/fmats.2022.1071316

Overall feasibility assessment of polyester polyurethane concrete used as steel bridge deck pavement

Shi-Lei Niu[1], Jun-Yi Wang[2], Zuo-Cai Wang[1,3]*, Dong-Hui Wang[4], Xiao-Tong Sun[1] and Xi Zhao[1]

[1]Department of Civil Engineering, Hefei University of Technology, Hefei, China, [2]Ningbo Road Technology Industrial Group Co., Ltd., Ningbo, China, [3]Anhui Province Infrastructure Safety Inspection and Monitoring Engineering Laboratory, Hefei, China, [4]China Railway Major Bridge Reconnaissance & Design Institute Co., Ltd., Wuhan, China

Traditional pavement materials used in the orthotropic steel bridge deck suffer from various pavement distresses and thus reduce the service life of the steel bridge. Therefore, this study proposed a novel engineered material named polyester polyurethane concrete (PPUC) for the steel bridge deck pavement. Indoor laboratory experiments and numerical comparison analysis were conducted to comprehensively assess the feasibility of PPUC as the steel bridge deck pavement and ordinary Portland cement (OPC), guss asphalt concrete (GAC), asphalt mastic concrete (SMAC) and epoxy asphalt concrete (EAC) were used as references compared with PPUC. After the specimens of PPUC were prepared by mixing polyester polyurethane binder (PPUB) and aggregate with the binder-aggregate ratio of 15%, the specimens were subjected to compressive test, splitting tensile test, flexural tensile strength test, wheel tracking test, low-temperature cracking test, freeze-thaw splitting test, shear test and pull-out test. The mechanical performance comparison of different pavement structures with different materials was also analyzed using finite element analysis method. Results show that PPUC presents higher mechanical properties (compressive, tensile and flexural strength) compared to OPC, and it has good durability properties compared to SMAC, GAC, and EAC, such as high temperature stability, low temperature cracking resistance and water stability. In addition, PPUC has strong adhesive property with steel deck and does not change significantly with temperature changes. The finite element simulation results show that the maximum tensile strength and maximum compressive strength of PPUC in the single-layer structure are 0.51 MPa and 3.52 MPa respectively, which are much smaller than the experimental values and those of other materials. The maximum tensile strength and maximum shear strength of PPUC in the PPUC + SMAC composite structure are 0.232 MPa and 0.148 MPa respectively, which are also much smaller than the experimental values and those of other structures. The mechanical performance comparison results indicate that PPUC pavement structure can improve the overall stiffness of the steel bridge deck and protect the wear layer. These results support that the PPUC has a promising application for the steel bridge deck pavement.

KEYWORDS

polyester polyurethane concrete, steel bridge deck pavement, mechanical properties, durability properties, adhesive property, mechanical performance comparison

1 Introduction

The orthotropic steel bridge deck is widely used in the large-span steel bridge all over the world due to its light weight, large span capacity and comfortable driving performance (He et al., 2021; Huang et al., 2022; Liu G et al., 2022). However, the existence of transverse and longitudinal ribs has a significant impact on the force conditions of steel deck pavement. When the steel deck pavement is subjected to vehicle load, some harmful load effects such as negative bending moment, stress concentration and interface slip will be found at the corresponding position on the pavement (Kainuma et al., 2016; Ma et al., 2018). Besides, a greater deformation of pavement occurs on the orthotropic steel deck compared with the ordinary pavement built on solid subgrade (Luo et al., 2017). Therefore, the requirements for the steel bridge deck pavement material are more stringent than those of the ordinary road pavement with following properties: high strength, good deformation ability, good bonding ability, high temperature stability, low temperature crack resistance and durability (Shao et al., 2013; Zeng et al., 2022; Zhu et al., 2022).

At present, the asphalt mixtures are widely used as the pavement materials for the steel bridge deck comprising guss asphalt concrete (GAC), stone mastic asphalt concrete (SMAC) and epoxy asphalt concrete (EAC). However, they are highly sensitive to ambient temperature, displaying viscoelasticity and brittleness at high and low temperature respectively, leading to a variety of surface damages such as cracking, rutting, pushing, and potholes etc. (Ma et al., 2018; Fan and Luo, 2021; He et al., 2021). For instance, GAC presents poor high temperature stability and is prone to rutting in spite of its excellent waterproof, anti-cracking and anti-aging properties. SMAC with good flexibility, anti-cracking and permanent deformation resistance presents an insufficient bond strength between the pavement and the steel bridge deck (Jiang et al., 2020; Liu Y et al., 2022). EAC shows high strength, relatively strong high-temperature stability, low-temperature crack resistance and permanent deformation ability. Moreover, it also has certain ability to resist fatigue and chemical erosion. However, the preparation process is complicated due to the strict controls of time and temperature in construction and the material cost of EAC is high (Chen C et al., 2018; Jiang et al., 2020; Liu Z et al., 2022). Therefore, there is an unmet need to develop a novel material formulation and a pavement structure, prolonging the service life of steel deck pavement (Alrefaei and Dai, 2022).

Polyurethane, produced by the reaction of multiorganic isocyanate and various hydrogen donors, contains various carbamate groups (-NHCOO-) on the main chain of the macromolecular structure, presenting superior properties of wear resistance, high temperature resistance, good mechanical properties and excellent adhesive ability (Jiang et al., 2020; Xu et al., 2020; Alrefaei and Dai, 2022). Moreover, it is highly flexible and elastic, which can be subjected to a greater deformation. Therefore, it is highly relevant to use as a paving material to increase the service life of steel bridge deck (Jiang et al., 2020; Meng et al., 2021). In recent years, polyurethane concrete has been gradually applied to bridge pavement engineering. Ningbo Lubao Company has developed polyester polyurethane concrete (PPUC), which has good durability, strong adhesion with steel, early strength, low temperature workability, etc. At present, PPUC has been applied to many bridge projects in China. In addition, PPUC is easily prepared at the room temperature and contributes to the carbon emissions reduction, thus protecting the environment (Xu et al., 2020).

In recent years, the polymer concrete has received increasing attention, designating to the term of cement concrete materials mixed with polymer materials. J.P. Romualdi et al. mixed steel fiber and concrete to form a steel fiber polymer concrete with good bending resistance for enhancing durability of steel structure. But its flexibility is too poor to ensure the coordinated deformation of steel bridge surface and pavement (Han et al., 2014; Kim et al., 2014; Romualdi and Mandel, 2021). Song et al. produced a polymer alloy material by mixing different kinds of polymers with concrete to produce polymer alloy material in a laboratory scale. Results showed that the developed composite exhibited properties of light and high-strength, good bonding performance and high-temperature performance Song et al. (2012). Yang et al. (2020) developed polyurethane void elastic pavement with the good rutting resistance. Hong et al. introduced polyurethane-based friction courses and polyurethane concrete suitable for tunnel pavement. Results indicated that they had excellent mechanical and functional properties Hong et al. (2020). Lu et al. produced polyurethane concrete with great waterproofing property by comparatively adjusting the aggregate gradation and discovered that it had good on-road performance and durability Lu et al. (2019). Chen J et al. (2018) studied the frost resistance of polyurethane concrete and discovered that polyurethane concrete could significantly postpone the ice generation procedure. Li et al. (2019) studied the difference between high performance polyurethane pervious mixture and porous asphalt mixture from aspects of mechanical properties, functional properties and void microscopic characteristics through indoor tests and found that the former had excellent mechanical and functional properties. Wang et al. (2014) investigated the characteristics of strength and road performance of porous polyurethane macadam mixture, and analyzed the temperature impacts on its strength and

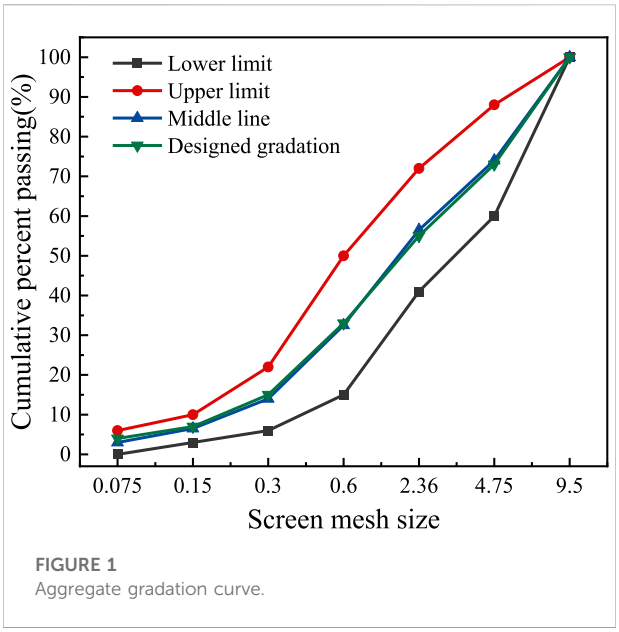

FIGURE 1
Aggregate gradation curve.

deformation resistance. Wang et al. (2017) developed a porous elastic pavement using polyurethane, which exhibited good noise reduction properties, superior low temperature tensile properties, anti-abrasion resistance and rutting resistance. Cong et al. (2018) conducted experimental studies on the basic properties of polyurethane binders and polyurethane permeable mixtures and analyzed the effect of immersion damage on the mixtures. These studies indicate that polyurethane mixtures, with good mechanical properties and high temperature characteristics, are promising candidate materials for the pavement applications.

In this study, PPUC was used as the pavement material for the steel bridge deck. The characteristics of PPUC were comprehensively investigated and compared with the traditional asphalt mixture (GAC, SMAC and EAC) and ordinary Portland cement (OPC). The structure of this paper is as follows. Firstly, the PPUC specimens were prepared. Then, the mechanical property test, wheel tracking test, low-temperature bending test and freeze-thaw splitting test were carried out to evaluate the characteristics of the material, followed by the evaluation of shear test and pull-out test (Munoz et al., 2014). Finally, the numerical simulation was implemented to compare mechanical performance of different pavement structures with different materials.

2 Material performance test

2.1 Raw materials and specimen preparation

PPUC, a thermosetting mixture, was prepared by mixing polyester polyurethane binder (PPUB) and a certain gradation of aggregate at room temperature. The compressive test was used for the optimum binder-aggregate ratio design. According to the test results, the optimum proportion of binder and aggregate was obtained as 15%–17%. In this study, 15% was determined as the optimum binder-aggregate ratio. Aggregate, as an important component of concrete, was used to enhance the mechanical properties of concrete. In this study, natural sand and natural gravel were used as aggregates, with the nominal particle of 0.075–4.75 mm and 4.75–9.5 mm respectively. The gradation of the aggregate is presented in Figure 1. The technical properties of the PPUB and the aggregate are shown in Table 1.

PPUC standard specimens of different sizes were prepared following the Standard for Test Methods of Physical and Mechanical Properties of Concrete (GB/T50081-2019, 2019) and the Test Procedure for Asphalt and Asphalt Mixture for Highway Engineering (JTG E20-2011, 2011). The preparation of PPUC specimens was clearly specified as follows: after mixing the aggregates uniformly according to the design gradation, they were added to the concrete experimental mixer and mixed in a dry state at room temperature for 3 min. Then PPUB was evenly mixed with the aggregate for 3 min. And then, the fresh PPUC mixture was cast into the mold to prepare PPUC specimens with different dimensions and all specimens were cured at room temperature for 24 h. Finally, all specimens were demolded and then maintained at a temperature of 20 ± 2°C before the tests. The relevant test items and specimen dimensions are shown in Table 2.

GAC, EAC, and SMAC are commonly used as bridge deck materials which consist of asphalt, aggregate and mineral powder. In this study, composite modified asphalt (80% SBS modified asphalt + 20% TLA lake asphalt), epoxy asphalt and SBS modified asphalt were used to prepare the asphalt mixture (GAC, EAC and SMAC, respectively). The basalt with a good angular performance was chosen as the coarse and fine aggregate. Limestone mineral powder was used as a filler to stabilize the internal concrete structure. The performance indicators of the raw materials all meet the requirements of the JTG E20-2011 and the Technical Specification for Design and Construction of Highway Steel Bridge Deck Pavement (JTG/T3364-02-2019, 2019). GAC, EAC were prepared using AC-10 gradation and SMAC were prepared using AC-13 gradation.

2.2 Mechanical properties test

The mechanical properties of PPUC were mainly assessed by compressive strength, tensile strength and flexural tensile strength and compared with those of ordinary Portland cement (OPC) (Zhang et al., 2020a). A cube specimen of 150 mm × 150 mm × 150 mm was subjected to a universal testing machine with the loading rate of 0.5 MPa/s for the compressive test as shown in Figure 2A. The tensile strength of PPUC was indirectly measured by splitting tensile test. Typically, the splitting strength is higher than the direct tensile strength. The specimen with dimension of

TABLE 1 Technical properties of the PPUB and the aggregate.

Test items	Technical properties	Test results	Technical requirements	Test method
PPUB	Tensile strength (MPa)	15.7	≥10	GB/T1040
	Fracture elongation (%)	34	≥25	GB/T1040
	Thermosetting property (300°C)	No melting	No melting	GB/T30598
	Water absorption (%)	0.1	≤0.3	GB/T1034
Aggregate	Density (g/cm^2)	2.62	≥2.4	T0304
	Water absorption (%)	1.3	≤2.0	T0304
	Moisture content (%)	0.25	≤0.3	T0305
	Firmness (%)	8	≤12	T0340

TABLE 2 Specimen dimensions in different test items.

Experimental items	Test method	Dimension/mm	References specification
Compressive strength	Cube compressive strength test	150 × 150 × 150	GBT 50081
Tensile strength	Splitting tensile test	150 × 150 × 150	GBT 50081
Flexural tensile strength	Four-point bending test	150 × 150 × 550	GBT 50081
High-temperature stability	Wheel tracking test	300 × 300 × 50	JTG E20-2011
Low-temperature crack resistance	Three-point bending test	250 × 30 × 35	JTG E20-2011
Water stability	Freeze-thaw splitting test	ϕ101.6 × 63.5	JTG E20-2011

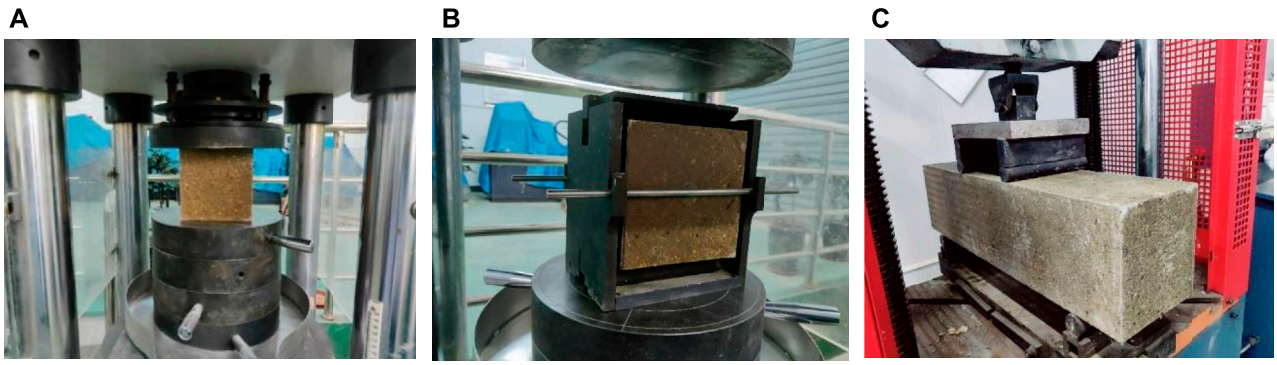

FIGURE 2
Mechanical properties test procedure. **(A)** Compressive test, **(B)** Splitting tensile test, **(C)** Flexural tensile test.

150 mm × 150 mm × 150 mm was placed on a special clamp and applied with a loading rate of 0.08 MPa/s (Figure 2B). The specimen of 150 mm × 150 mm × 550 mm was performed by the flexural tensile strength test with the bottom supported and restrained. The distance between the two supports was 450 mm, and the length of the pure bending section was 150 mm. The loading rate in the test was determined as 0.5 MPa/s. The test process is shown in Figure 2C.

As shown in Table 3, the mechanical properties of PPUC with compressive strength of 75.3 MPa, splitting tensile strength of 8.4 MPa and flexural tensile strength of 22.4 MPa are significantly higher than those of OPC and allocated in C70 strength grade, suggesting promising basic mechanical properties for the steel bridge deck pavement. The damage of the concrete sample is mainly attributed to the growth of microcracks in the matrix, which may lead to the failure of the concrete. Similar to

TABLE 3 Mechanical properties.

Material	Compressive strength (MPa)	Splitting tensile strength (MPa)	Flexural tensile strength (MPa)
PPUC	75.3	8.4	22.4
OPC	32.1	1.8	4.2

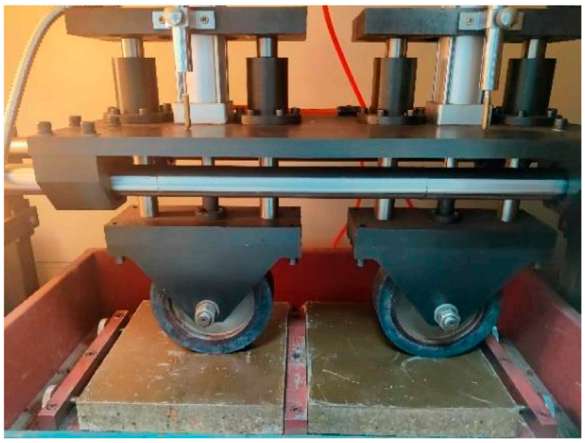

FIGURE 3
The schematic diagram of the gradient concrete test block.

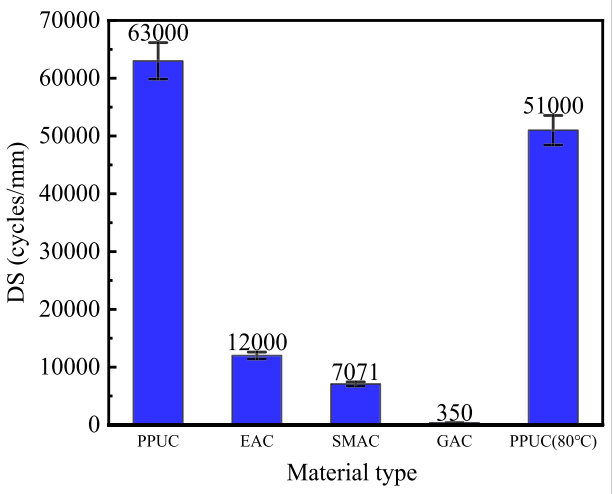

FIGURE 4
Wheel tracking test result.

the rubber concrete, PPUC is stiffened by the well-dispersed fine elastomeric resins. When the structure is deformed by the external forces, the elastomeric resin helps to resist cracking (Cai et al., 2012; Ho et al., 2012; Wang et al., 2019).

2.3 Wheel tracking test

The temperature of steel bridge decks can reach up to 70°C in summer, which has a significant influence on the service life of paving material (Luo et al., 2017; W. and L., 2012). In this sense, wheel tracking test was performed to evaluate the ability of PPUC resisting the repeated loading temperature of 60°C (Figure 3). The dynamic stability (DS) was used as the evaluation index. Briefly, the concrete specimens with dimensions of 300 mm × 300 mm × 50 mm were subjected to wheel tracking tests by following T0719-2011 (JTG E20-2011, 2011). The test wheel tires were made of solid rubber with an outer diameter of 200 mm and a wheel width of 50 mm. The rubber tires pressure was designed as 0.7 ± 0.05 MPa, and the speed of rolling back and forth was 42 times/min. The rutting specimens were fixed on the operating platform in the test box and the internal temperature was maintained at 60°C throughout the test.

The larger DS indicates the greater ability of concrete material to resist the rutting deformation and the DS of pavement material is required to be larger than 3500 cycles/mm. In this study, the DS of EAC, SMAC, and GAC were also measured for the comparison. It can be observed in Figure 4 that the DS values of both PPUC and EAC are larger than 10000 cycles/mm while the DS of PPUC is about six times higher than that of EAC and significantly higher than that of SMAC and GAC respectively. Moreover, the decrease of DS for PPUC (19%) is smaller than that of EAC, SMAC and GAC respectively in case of high temperature at 80°C. The rutting depth of the PPUC under the wheel-track loading is neglectable indicating the little rutting deformation occurred. It is mainly due to the higher rigidity and elastic resilience of the polyurethane binder that helps the PPUC specimens to resist the rutting deformation (Jiang et al., 2020).

2.4 Low-temperature bending test

The shrinkage deformation in the road surface and tensile stress generated in the inner pavement layer at a low temperature may allow the pavement layer susceptible to temperature shrinkage cracks (Liu G et al., 2022). Due to the high elastic modulus of PPUC, a large temperature stress will be generated as the temperature drops, which will easily cause crack-ing. Following the T0715-2011 (JTG E20), the bending beam test was performed at −20°C and -10°C

FIGURE 5
Low-temperature bending test procedure.

respectively to evaluate the low temperature crack resistance of PPUC as shown in Figure 5. Maximum bending and tensile strain (MBTS), bending and tensile strength modulus (BTSM) and bending and tensile strength (BTS) were used as evaluation indexes. Specimens with dimensions of 250 mm × 30 mm × 35 mm were assessed with the loading rate of 50 mm/min.

As presented in Figure 6, results show that the MBTS of PPUC (3545 με) is larger than those of EAC and SMAC (2706 and 2893με, respectively), indicating PPUC presents a better low-temperature resilience. Moreover, there is no significant difference between the MBTS values of PPUC at -10°C and -20°C (3545 and 3048με, respectively) suggesting that PPUC is less sensitive to a low temperature. The BTSM of PPUC is much close to that of EAC and dramatically larger than that of SMAC indicating that the two types of concrete with higher elastic modulus are prone to higher temperature stresses with the decrease of temperature. As for the BTS value, it can be seen that PPUC shows a higher value than EAC and about 2 times higher than SMAC, implying that PPUC exhibits better low-temperature strength. These results show that PPUC can reduce the probability of crack generation and deformation extension under the low temperature condition, and improve the durability of paving materials.

2.5 Freeze-thaw splitting test

The moisture in the pavement reduces the adhesion of PPUC binder and aggregate. Therefore, after being subjected to the repeated tests of traffic loads and temperature changes, the pavement will suffer from diseases such as extrusion deformation and pits. Referring to the test procedure of T0729-2011 (JTG E20), the freeze-thaw splitting test was implemented to evaluate the water damage resistance of PPUC. In this test, a cylindrical specimen with a diameter of 101.6 ± 0.25 mm and a height of 63.5 ± 1.3 mm was formed by the Marshall compaction method and performed the freeze-thaw cycling by the freeze-thaw testing machine. After that, the specimens were placed on the splitting tester with a loading rate of 50 mm/min, as presented in Figure 7. The freeze-thaw splitting tensile strength ratio (STSR) of the specimens before and after the water damage was measured to evaluate the water stability of PPUC.

As shown in Table 4, it can be observed that the splitting strength of PPUC before and after the freeze-thaw cycling are significantly higher than those of EAC and SMAC (7.85 and 7.30 MPa respectively), indicating PPUC has a greater indirect tensile strength compared to SMAC and particularly EAC which is usually considered to be a thermosetting paving material with good water stability. It can be also found that the STSR of PPUC (93%) is larger than that of EAC (83%). The STSR of SMAC (95%) is greater than that of PPUC due to the addition of modifier, which improves the resistance of SMAC to water damage. These results show that PPUC has a good stability performance as the steel bridge deck pavement material under the coupling effect of water vapor and temperature.

3 Pavement structure performance test

3.1 Shear test

The failure of interface shear between the pavement and the steel deck is one of the main reasons for the deterioration of steel deck pavement quality (Zhang et al., 2020b; Lu et al., 2021; Majumder and Saha, 2021; Guan et al., 2022). Therefore, the shear strength between PPUC and steel plate was measured by the 45° oblique shear test, as illustrated in Figure 8. The specimen with the size of 100 mm × 100 mm × 40 mm was assessed by the oblique shear test using the loading rate of 10 mm/min. Moreover, in order to investigate the effect of temperature on the bonding layer, the shear test was conducted using two temperature configurations: room temperature (25°C) and high temperature (70°C) respectively. SMAC and EAC were used as control groups. The shear strength was calculated by Eq. 1:

$$\tau = \frac{F \times \sin\alpha}{S} \quad (1)$$

Where τ is the shear strength, F is the ultimate load when the specimen is damaged, S is the shear area of the specimen, and α is the shear angle at 45°.

Results show that the shear failure occurs at the interface between the PPUC and the steel plate at both the room

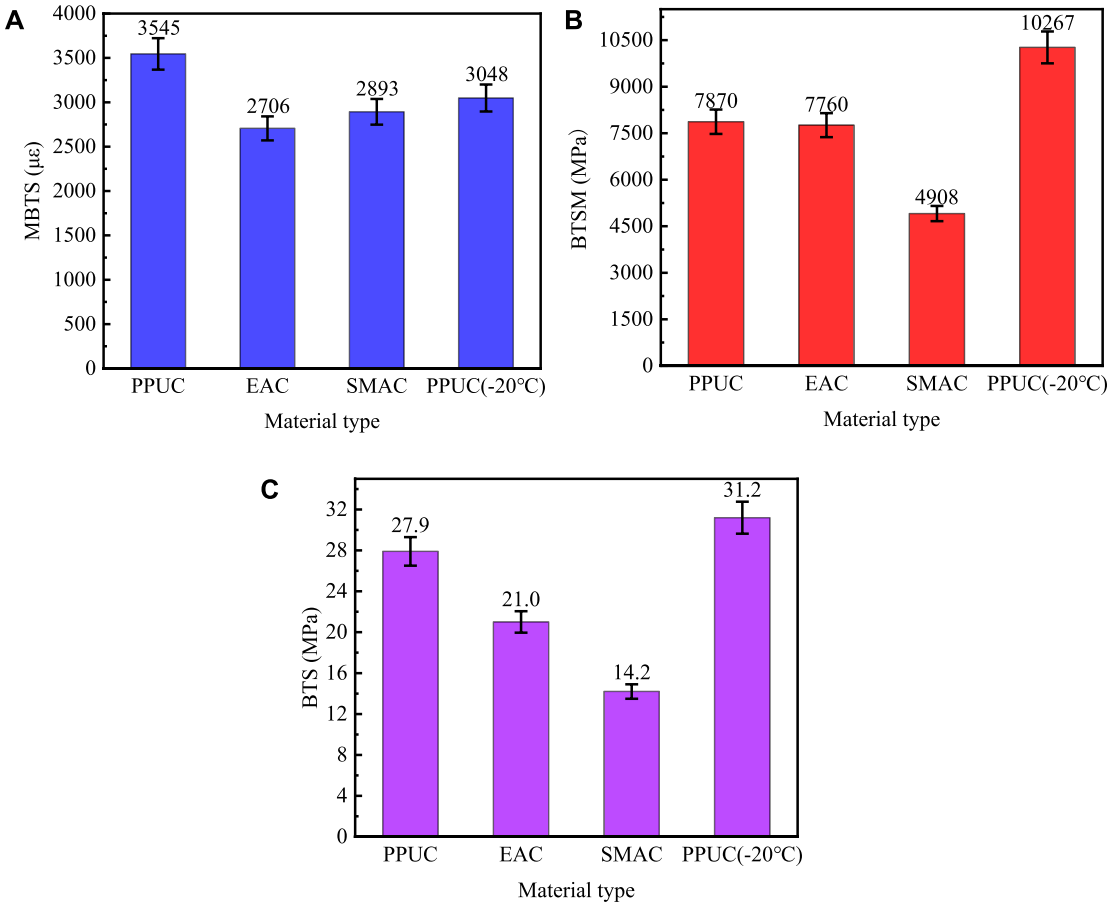

FIGURE 6
Low-temperature bending test results. **(A)** MBTS, **(B)** BTSM, **(C)** BTS.

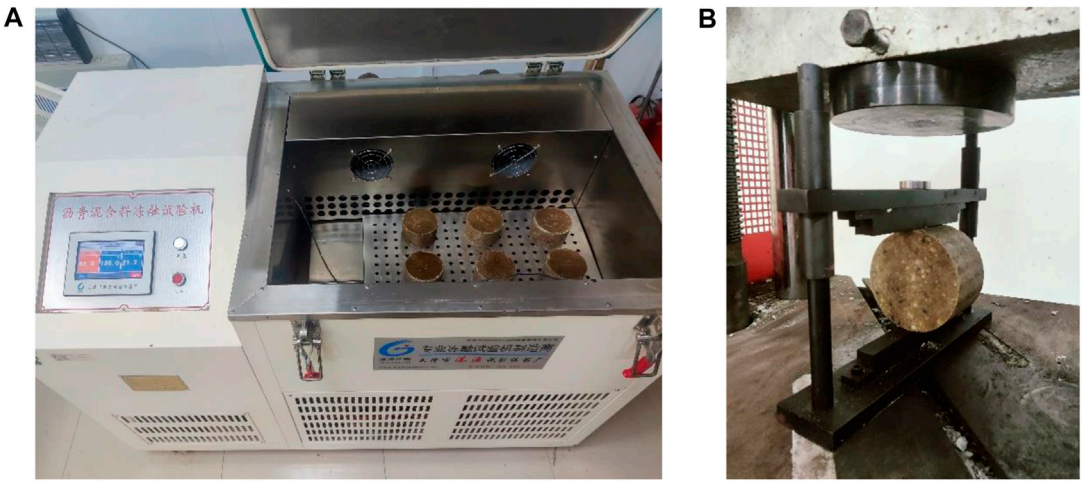

FIGURE 7
Freeze-thaw splitting test procedure. **(A)** Freeze-thaw cycle procedure; **(B)** Splitting test.

TABLE 4 The results of the freeze-thaw splitting test.

Material type	Strength before freeze-thaw (MPa)	Strength after freeze-thaw (MPa)	STSR (%)
PPUC	7.85	7.30	93
EAC	5.24	4.37	83
SMAC	1.57	1.49	95

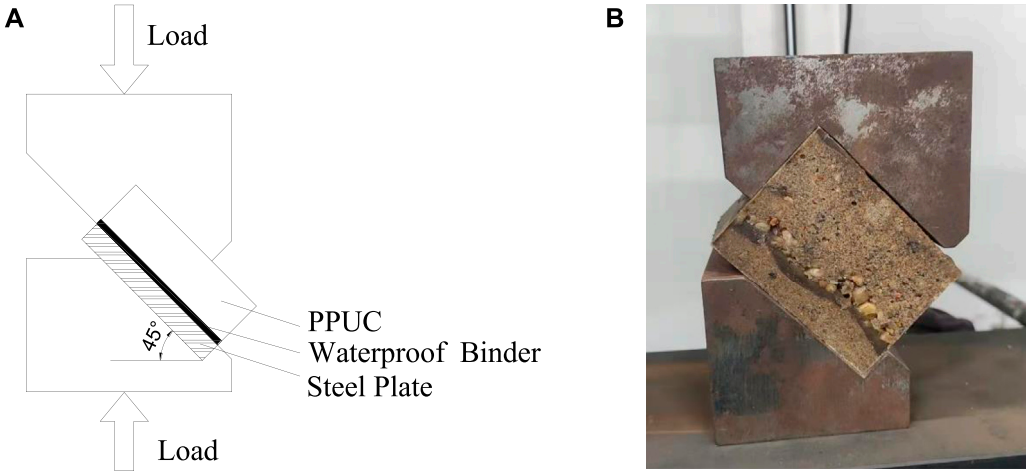

FIGURE 8
Shear test procedure. **(A)** Schematic of the shear test; **(B)** Test photo of the shear test.

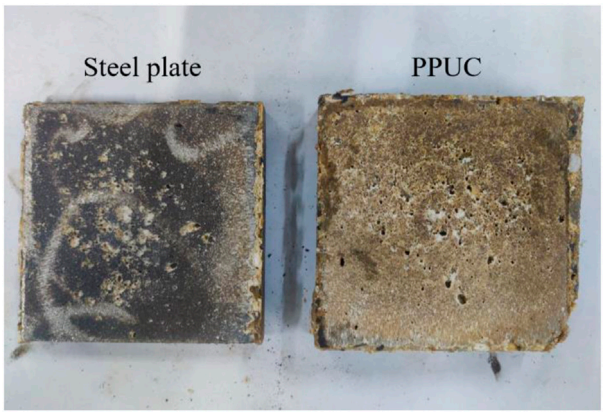

FIGURE 9
Failure mode of shear test.

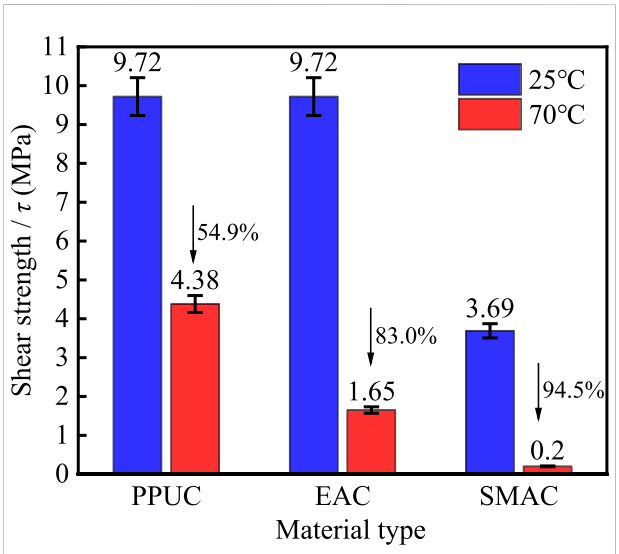

FIGURE 10
Shear test results.

temperature and high temperature condition, indicating the measured damage stress is the bond layer shear strength. The failure mode of the specimen is shown in Figure 9. Results in Figure 10 also show that the shear strength of PPUC (9.72 MPa) is same as that of EAC and much greater than that of SMA (3.69 MPa). With the temperature increase up to 70°C, all specimens exhibit a decreasing trend in terms of shear strength. However, PPUC shows the minimum variation of

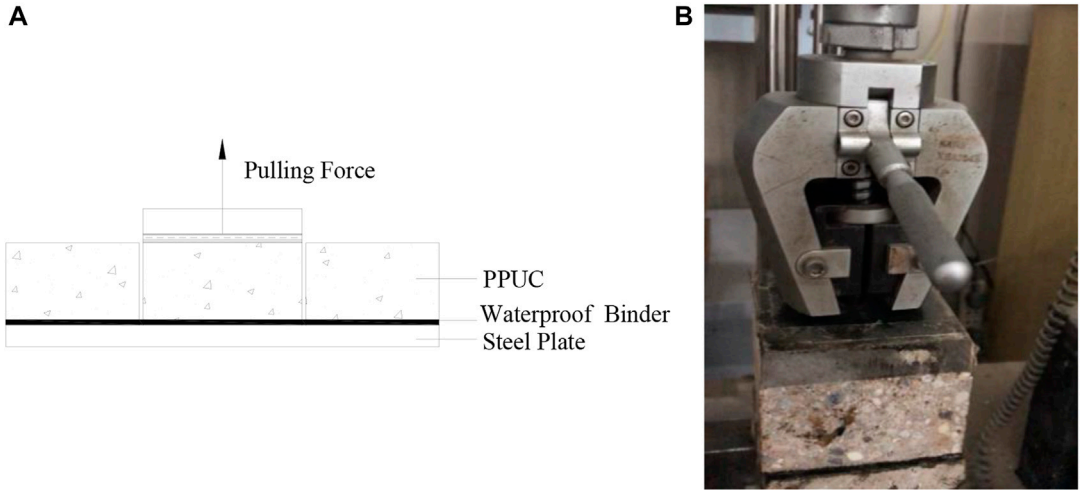

FIGURE 11
Pull-out test procedure. **(A)** Schematic diagram of the pull-out test; **(B)** Test set up of the pull-out test.

shear strength decreasing rate (54.9%) comparing with EAC and SMAC (83.0% and 94.5%, respectively). This might be attributed to the thermosetting property of PU allowing PPUC more stable at the high temperature than asphalt materials.

3.2 Pull-out test

The pull-out test was performed to investigate the adhesive characteristic between specimens and steel plate. The specimen dimension and test method were same as those of the oblique shear test. The specimens were bonded with a special jig using epoxy resin and performed the pull-out tests after the epoxy resin was completely cured for 24 h at 25°C and 70°C respectively. The schematic and experimental set-up is shown in Figure 11. The samples were applied with the vertical tensile force with a uniform rate of 10 mm/min until they braked and the maximum load was read. The condition of the fracture surface was observed and the failure location was also recorded. The pull-out strength was calculated by Eq. 2:

$$P = \frac{F}{S} \tag{2}$$

Where P is the pull-out strength, F is the ultimate load when the specimen is damaged, and S is the bottom surface area of the pull-out jig.

In this test, the failure surface is also located at the interface between the steel plate and PPUC pavement, suggesting the damage stress is the interlayer bond strength. Its failure mode is shown in Figure 12. Figure 13 also shows that the pull-out strength between PPUC and the steel plate (6.23 MPa) is 1.3 times higher than that of EAC (4.83 MPa), and significantly higher than that of SMA

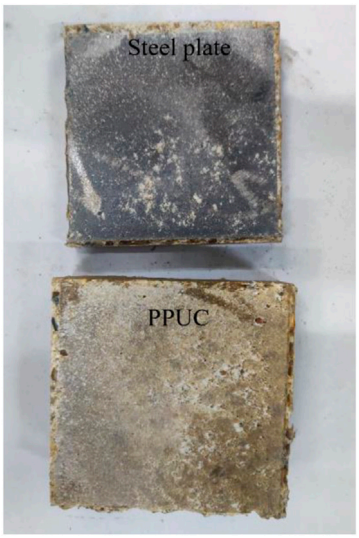

FIGURE 12
Failure mode of pull-out test.

(1.92 MPa) at room temperature of 25°C, indicating that PPUC has strong bond strength with the steel plate. In addition, as the temperature increases to 70°C, the pull-out strength of PPUC, EAC and SMA decreases by 29.2%, 72.5% and 80.7%, respectively. Similar to the shear strength, it can be attributed to the fact that the thermosetting property of PPUC makes its pull-out strength (4.41 MPa) higher at high temperature of 70°C. These results show the minimum difference of PPUC pull-out strength switching from room temperature to high temperature and higher bond strength of PPUC maintained at high temperature compared with other paving materials.

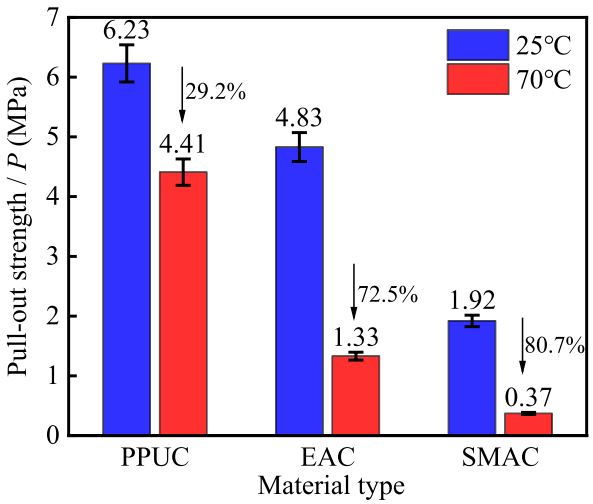

FIGURE 13
Pull-out test results.

4 Mechanical performance comparison of different pavement structures

4.1 Finite element model of the pavement structure

In this study, the model of the pavement structure was established based on three basic assumptions (Ma et al., 2018). 1) the pavement material is an isotropic material. 2) the interface of pavement layer is continuous. 3) the weight of steel deck and pavement is ignored.

The model was consisted of eight U-shaped stiffeners and four transverse diaphragms, as shown in Figure 14. The eight-node hexahedral linear reduction integral solid element (C3D8R) was used for steel deck and pavement. The mesh size was chosen to be 50 mm and the whole model was discretized into a total of 95020 elements. The interfaces of pavement layer were all defined as continuous, which means that a perfect bond was assumed at the interfaces in the finite element analyses. So, the binder layer was not specifically treated in the calculation and was considered in the bridge deck pavement. In addition, since the thickness of the waterproof bonding layer was negligible compared with that of the pavement layer, the waterproof bonding layer was not set in this model. The interlayer contact state was set to "Tie connection" for constraining the relative deformation and movement between two adjacent surfaces. The relevant geometric and material parameters of the pavement structure model are shown in Table 5 (Ma et al., 2018) and Table 6 (Li et al., 2013; Xue et al., 2020; Lv et al., 2021; Wang et al., 2021). The beam was simply supported at both ends and the bottom of the transverse diaphragm was completely consolidated. Considering the local stress characteristics of orthotropic steel deck under loading, the influence of these constraints on the finite element analysis can be ignored.

According to the Technical Standard for Highway Engineering (JTG B01-2014, 2015), the steam-overload 20 level was used as the calculated load. The simulated test load was designated as 0.758 MPa after considering 30% impact effect. The contact area between wheel and pavement was a rectangular plane of 600 mm × 200 mm. The position of wheel load has a great impact on the mechanical properties of steel deck pavement. Therefore, in order to determine the most unfavorable load position, different load conditions were tested along with the transverse and longitudinal directions shown in Figure 15. Three

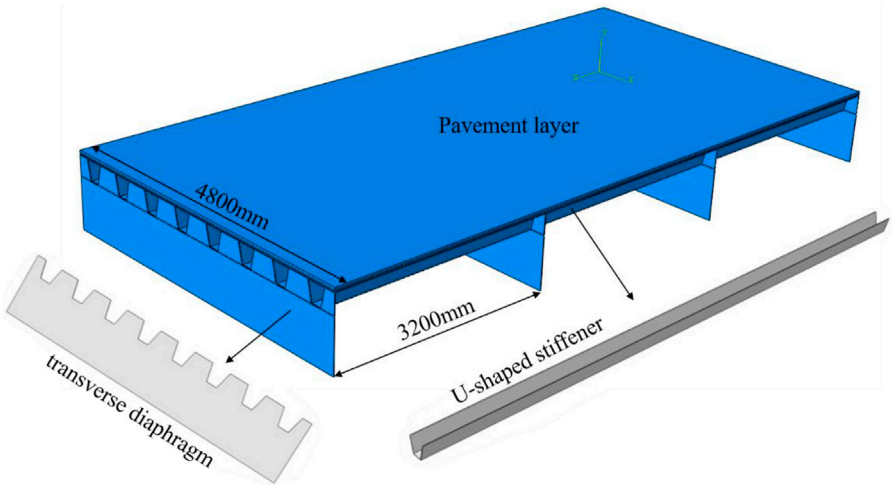

FIGURE 14
Finite element model of the pavement structure.

TABLE 5 Geometric parameters of the pavement structure model.

Geometric parameters	Value (mm)
Steel deck thickness	14
Diaphragm plate thickness	10
Diaphragm plate height	1000
Diaphragm plate spacing	3200
Stiffener thickness	8
Top width of stiffener	300
Bottom width of stiffener	170
Stiffener height	280
Stiffener spacing	600
PPUC overlay thickness (Composite pavement)	20
SMAC overlay thickness (Composite pavement)	30
PPUC overlay thickness (Single-layer pavement)	40

TABLE 6 Material parameters of the pavement structure model.

Material type	Elastic modulus (MPa)	Poisson ratio
PPUC	16000	0.3
SMAC	2020	0.3
EAC	4500	0.3
GAC	5000	0.3
Steel	210000	0.25

transverse load positions were considered in Figure 15A: Load I, the wheel pressure center acts on the midpoint of a stiffener; Load II, the wheel pressure center acts on the midpoint of two adjacent stiffeners; Load III, the wheel pressure center acts on the midpoint of one side of the stiffener. Figure 15B shows these three transverse loads move longitudinally from the midspan to the transverse diaphragm with intervals of 200 mm. There are totally nine longitudinal load positions labeled as Load 1 to 9.

4.2 Analysis of the most unfavorable load position

A single-layer PPUC pavement structure was selected to determine the most unfavorable load position of the steel bridge deck pavement. The maximum transverse tensile stress and the maximum vertical displacement of the paving layer were chosen as the verification indexes and their variation pattern is shown in the Figure 16. It can be observed that the longitudinal load position variation has a significant effect on the mechanical response of the pavement structure. With the decrease of distance between the load position and the transverse diaphragm, the maximum transverse tensile stress and the maximum vertical displacement of the paving layer are significantly decreased. Both the two verification indexes reach to the maximum value when the load is applied on the midspan of the steel bridge panel (Load 1). In the direction of the transverse bridge, two maximum values are reached when the load is applied on the midpoint of two adjacent stiffeners (Load II). Therefore, Load 1 and Load II are the most unfavorable load positions of the steel deck pavement structure.

4.3 Comparison of single-layer pavement structure

PPUC, SMAC, GAC and EAC were selected as the pavement materials for the single-layer pavement structure comparison. The midspan crossbridge direction distance was selected as the comparison route and the comparison results are shown in Figure 17 when the wheel load is applied to the most unfavorable load position.

Figures 17A, B show the vertical displacement of the pavement and steel bridge deck at the comparison route. It can be seen that the vertical displacement of pavement is minimal when the PPUC is used as the steel deck pavement material with the maximum displacement value of 0.583 mm. Similarly, the vertical displacement of the steel bridge deck (0.58 mm) is also minimal. Results also show that the vertical displacement of the pavement and steel bridge deck presents a decreasing trend with the increase of the pavement material elastic modulus.

Figure 17C presents the variation of transverse stress in the pavement over the comparison route. The larger elastic modulus of PPUC enables it to bear a greater stress. The maximum transverse compressive stress occurs at the most unfavorable load position, and the maximum transverse tensile stress occurs at the spot of 800 mm far from the middle of transverse span. The value of the maximum transverse tensile stress (0.51 MPa) of PPUC is less than the tensile strength obtained from the test (8.4 MPa). Similarly, the value of the maximum transverse compressive stress of PPUC (3.52 MPa) is less than the test value (75.3 MPa). The Mises stress distribution of steel bridge deck is shown in Figure 17D. Two stress concentration phenomena are observed in the steel bridge deck with SMAC, GAC and EAC pavement layers with the maximum Mises stress values over 8 MPa in these two locations. However, the use of PPUC pavement structure improves the stress on the steel bridge deck and reduces the number of stress concentration locations and the maximum stress amplitude. The maximum Mises stress occurred at the most unfavorable load position of the steel bridge deck for PPUC (7.89 MPa) is significantly smaller than those of the steel bridge deck with other three pavement structures. These

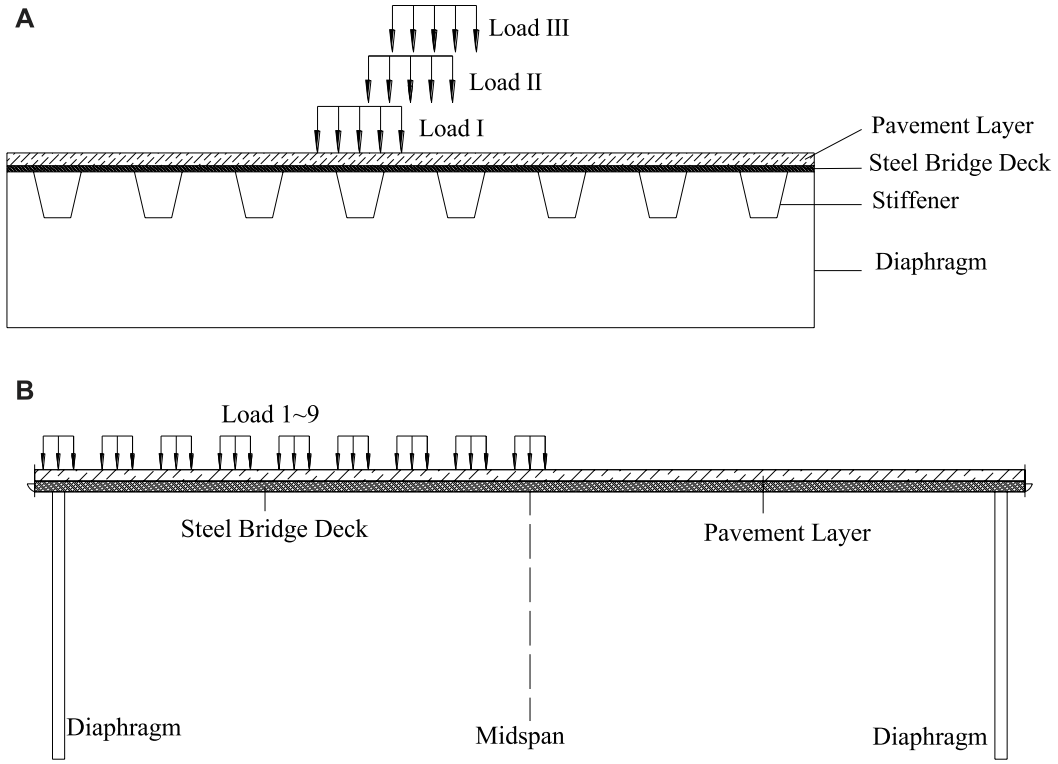

FIGURE 15
Load distribution on the pavement structure. **(A)** Transverse load distribution; **(B)** Longitudinal load distribution.

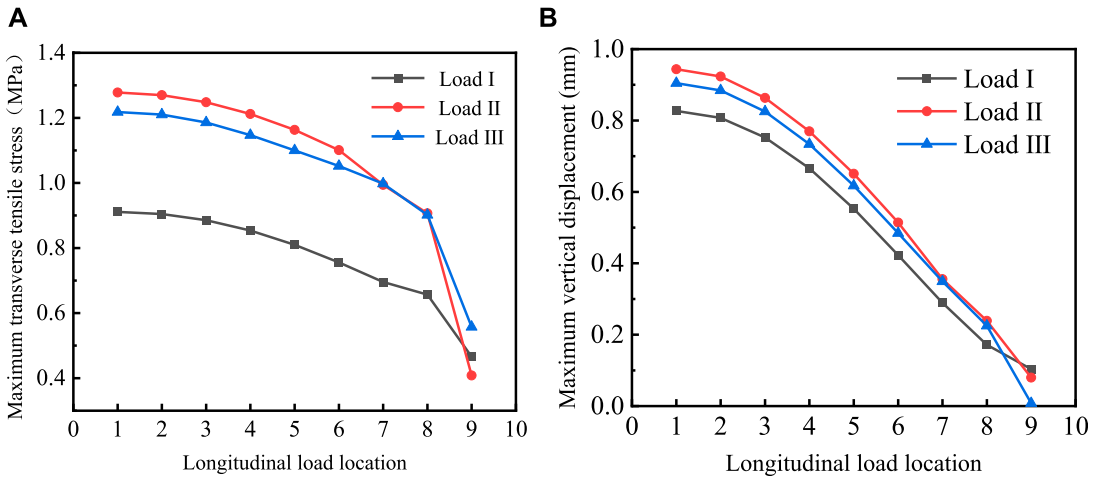

FIGURE 16
Analysis of the most unfavorable load position. **(A)** Maximum transverse tensile stress of the pavement; **(B)** Maximum vertical displacement of the pavement.

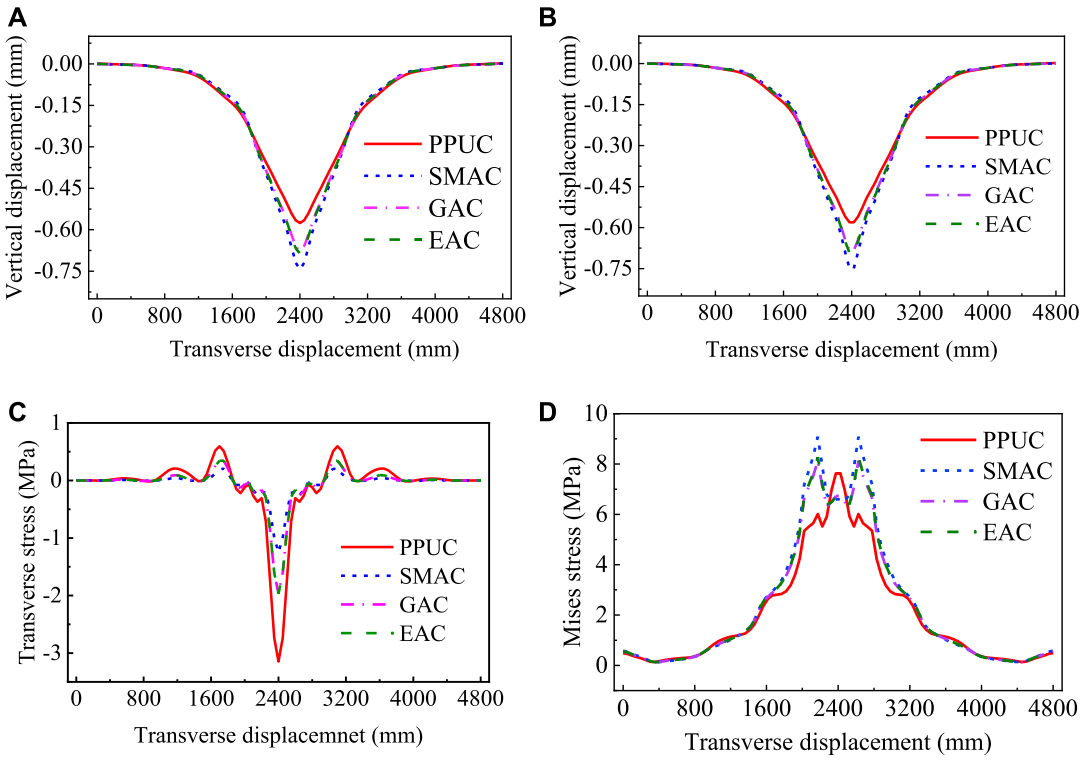

FIGURE 17
Comparison results of single-layer pavement structure using different materials. **(A)** Vertical displacement of the pavement; **(B)** Vertical displacement of the steel deck; **(C)** Transverse tensile stress of the pavement; **(D)** Mises stress of the steel bridge deck.

results indicate that the PPUC pavement layer contributes to distributing the stress on the steel bridge deck and improving the overall stiffness of the steel bridge deck.

4.4 Comparison of composite pavement structure

As for the composite pavement structure, the SMAC was used as the upper layer material and the PPUC, GAC and EAC were used as the lower layer materials. Therefore, there are three kinds of composite pavement structures: PPUC + SMAC, GAC + SMAC, EAC + SMAC. The comparison results are shown in Figure 18.

Figure 18A shows the maximum transverse tensile stress of the pavement. Results show that the PPUC pavement structure presents the smallest value of the maximum transverse tensile stress in terms of the upper layer (0.2316 MPa) while that of the lower layer is the largest (0.649 MPa) compared to other two composites. It can be concluded that the maximum transverse tensile stress in the lower layer decreases while that in the upper layer increases with the elastic modulus of lower layer material decreasing. The longitudinal cracking in the wear layer is one of the most common pavement distresses for the steel bridge deck pavement. Excessive transverse tensile stresses can easily contribute to the generation of longitudinal cracks, and subsequently damaging the steel bridge deck. The use of PPUC makes the maximum transverse tensile stress in the upper layer smaller, which reduces the generation and development of longitudinal cracks. The larger shear stress that occurs inside the pavement layer can cause shear damage, which produces the pavement distresses of slippage and swell. It can be seen from Figure 18B that the maximum longitudinal shear stress variation pattern of the upper and lower layers in the composite pavement structure is similar to that of the tensile stress and the PPUC pavement layer bears more tensile and shear stresses, contributing to the protection of the upper layer and minimizing the pavement diseases occurred in the upper layer. This result indicates that the use of PPUC reduces the yield stress of steel bridge deck.

Figure 18C demonstrates the maximum Mises stress variation pattern for the lower layer and steel bridge deck. With decreasing the elastic modulus of the lower layer pavement material, the maximum Mises stress in the lower layer gradually decreases while that in the steel bridge deck increases. Figure 18D presents the maximum vertical

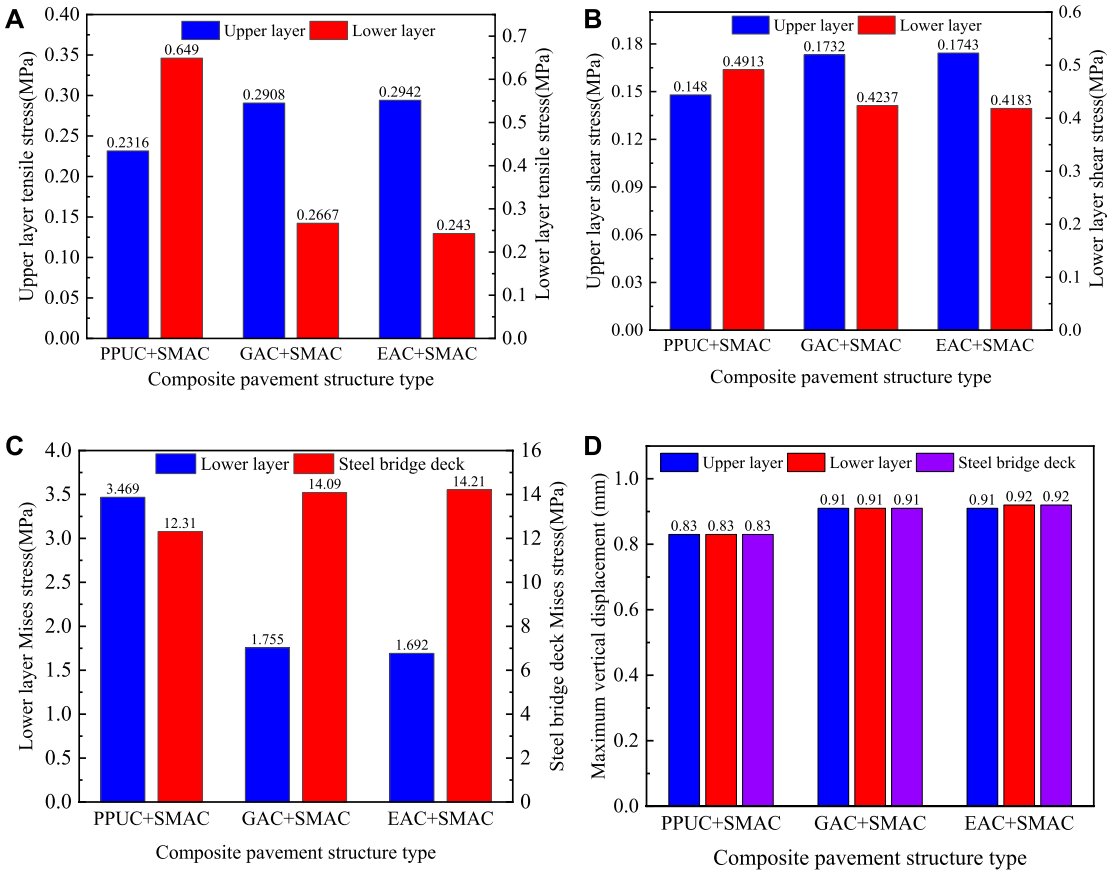

FIGURE 18
Comparison results of different composite pavement structures. **(A)** Maximum transverse tensile stress of the pavement; **(B)** Maximum shear stress of the pavement; **(C)** Mises stress of the lower layer and steel bridge deck; **(D)** Maximum vertical displacement of the pavement and steel bridge deck.

displacement of the upper layer, lower layer and steel bridge deck respectively. Results show that the maximum vertical displacement of PPUC + SMAC pavement structure is the smallest among the three composite pavement structures. This indicates that the PPUC + SMAC pavement structure has better riding comfort under the same traffic load. The above results show that the PPUC pavement layer is beneficial to improve the overall stiffness of the steel bridge deck, reduce the maximum force on the steel bridge deck, protect the wear layer and extend the service life of the steel deck pavement structure.

5 Conclusion

In this paper, PPUC was proposed as the steel bridge deck pavement material. Its mechanical properties, durability and shear bond properties were comprehensively investigated by both the experiments and finite element analysis. In comparison, the commonly used steel bridge deck pavement materials including EAC, SMAC and GAC were also investigated as references. Based on the study results, the conclusions can be summarized as follows.

(1) PPUC presents large compressive, tensile and flexural tensile strength of 75.3, 8.4, and 22.4 MPa, respectively, which meet the strength demands of the steel bridge for the opening traffic and the subsequent service.
(2) The results of wheel tracking test, low-temperature bending test and freeze-thaw splitting test show that PPUC presents the better high temperature deformation resistance, low temperature cracking resistance and water stability performance compared to EAC, SMAC and GAC materials. Moreover, these properties are not significantly changed in the extreme severe environments, such as at high temperatures of 70°C, low temperatures of −20°C and cyclic freeze-thawing circumstances.
(3) According to the results of the shear test and the pull-out test, the oblique shear strength (9.72 MPa) and pull-out strength

(6.23 MPa) between PPUC and steel deck are greater than those of EAC and SMAC at 25°C. Moreover, the decrease of these strengths for PPUC at high temperature of 70°C is much smaller than that of the other two materials. These results indicate that the PPUC pavement structure has stronger bonding properties and resistance to the perpetual deformation.

(4) The finite element analysis results show that the most unfavorable load position of the steel deck pavement structure is Load II (the wheel pressure center acts on the midpoint of two adjacent stiffeners) and Load 1 (the wheel pressure center acts in the middle of the span). The PPUC single-layer pavement structure and the PPUC + SMAC composite pavement structure have better mechanical properties. Therefore, PPUC is a feasible material for the future steel bridge deck pavement.

Data availability statement

The raw data supporting the conclusion of this article will be made available by the authors, without undue reservation.

Author contributions

S-LN: Methodology, validation, data curation, writing—original draft; J-YW: Methodology, validation; Z-CW: Conceptualization, formal analysis, investigation, writing—review and editing; D-HW: Validation, data curation; X-TS: Vali-dation, data curation; XZ: Validation, data curation.

Funding

Financial support of this study was provided in part by the National Natural Science Foundation of China under grand Nos. 51922036 and 52278301, by the Fundamental Research Funds for the Central Universities under grand No. JZ2020HGPB0117, and by the Science Technology Research and Development Program Project of China Railway Group Co., Ltd. (2020-major-01). The results and opinions expressed in this paper are those of the authors only, and they don't necessarily represent those of the sponsors.

Conflict of interest

J-YW was employed by Ningbo Road Technology Industrial Group Co., Ltd.

D-HW was employed by China Railway Major Bridge Reconnaissance & Design Institute Co., Ltd.

The remaining authors declare that the research was conducted in the absence of any commercial or financial relationships that could be construed as a potential conflict of interest.

Publisher's note

References

Alrefaei, Y., and Dai, J. G. (2022). Effects of delayed addition of polycarboxylate ether on one-part alkali-activated fly ash/slag pastes: Adsorption, reaction kinetics, and rheology. *Constr. Build. Mat.* 323, 126611. doi:10.1016/j.conbuildmat.2022.126611

Cai, D., Jin, J., Yusoh, K., Rafiq, R., and Song, M. (2012). High performance polyurethane/functionalized graphene nanocomposites with improved mechanical and thermal properties. *Compos. Sci. Technol.* 72, 702–707. doi:10.1016/j.compscitech.2012.01.020

Chen C, C., Eisenhut, W. O., Lau, K., Buss, A., and Bors, J. (2018). Performance characteristics of epoxy asphalt paving material for thin orthotropic steel plate decks. *Int. J. Pavement Eng.* 21, 397–407. doi:10.1080/10298436.2018.1481961

Chen J, J., Xie, M., Hao, W., Xie, P., and Wei, H. (2018). Experimental study on antiicing and deicing performance of polyurethane concrete as road surface layer. *Constr. Build. Mat.* 161, 598–605. doi:10.1016/j.conbuildmat.2017.11.170

Cong, L., Wang, T. J., Tan, L., Yuan, J. J., and Shi, J. C. (2018). Laboratory evaluation on performance of porous polyurethane mixtures and OGFC. *Constr. Build. Mat.* 169, 436–442. doi:10.1016/j.conbuildmat.2018.02.145

Fan, X., and Luo, R. (2021). Experimental study on crack resistance of typical steel-bridge deck paving materials. *Constr. Build. Mat.* 277, 122315. doi:10.1016/j.conbuildmat.2021.122315

GB/T50081-2019 (2019). *Standard for test methods of concrete physical and mechanical properties*. Beijing: Ministry of housing and urban rural development of the people's Republic of China.

Guan, Y., Wu, J., Sun, R., Ge, Z., Bi, Y., and Zhu, D. (2022). Shear behavior of short headed studs in Steel-ECC composite structure. *Eng. Struct.* 250, 113423. doi:10.1016/j.engstruct.2021.113423

Han, B. J., Yoon, S. I., Choi, B. J., Choi, J. W., and Park, S. K. (2014). Analysis study on fatigue stress on the orthotropic steel deck applied polymer concrete pavement. *J. Korea Inst. Struct. maintenance Insp.* 18, 68–77. doi:10.11112/jksmi.2014.18.5.068

He, Q., Zhang, H., Li, J., and Duan, H. (2021). Performance evaluation of polyurethane/epoxy resin modified asphalt as adhesive layer material for steel-UHPC composite bridge deck pavements. *Constr. Build. Mat.* 291, 123364. doi:10.1016/j.conbuildmat.2021.123364

Ho, A. C., Turatsinze, A., Hameed, R., and Vu, D. C. (2012). Effects of rubber aggregates from grinded used tyres on the concrete resistance to cracking. *J. Clean. Prod.* 23, 209–215. doi:10.1016/j.jclepro.2011.09.016

Hong, B., Lu, G., Gao, J., Dong, S., and Wang, D. (2020). Green tunnel pavement: Polyurethane ultra-thin friction course and its perfor-mance characterization. *J. Clean. Prod.* 289, 125131. doi:10.1016/j.jclepro.2020.125131

Hong-Chang, W., and Guo-Fen, L. (2015). Study on high-temperature stability of composite gussasphalt concrete. *Mater. Res. Innovations* 19, S5-494–S5-499. doi:10.1179/1432891714z.0000000001139

Huang, Y., Chen, S., and Gu, P. (2022). Interface stress analysis and fatigue design method of steel-ultra high performance concrete composite bridge deck. *Structures* 38, 1453–1464. doi:10.1016/j.istruc.2022.03.005

Jiang, Z., Tang, C., Yang, J., You, Y., and Lv, Z. (2020). A lab study to develop polyurethane concrete for bridge deck pavement. *Int. J. Pavement Eng.* 23, 1404–1412. doi:10.1080/10298436.2020.1804063

JTG B01-2014 (2015). *Technical standard of highway engineering*. Beijing: Ministry of transport of the people's Republic of China.

JTG E20-2011 (2011). *Standard test methods of bitumen and bituminous mixtures for highway engineering*. Beijing: Ministry of transport of the people's Republic of China.

JTG/T3364-02-2019 (2019). *Technical specification for design and construction of highway steel bridge deck pavement*. Beijing: Ministry of transport of the people's Republic of China.

Kainuma, S., Yang, M., Jeong, Y.-s., Inokuchi, S., Kawabata, A., and Uchida, D. (2016). Experiment on fatigue behavior of rib-to-deck weld root in orthotropic steel decks. *J. Constr. Steel Res.* 119, 113–122. doi:10.1016/j.jcsr.2015.11.014

Kim, T., Baek, J., Lee, H. J., and Lee, S. Y. (2014). Effect of pavement design parameters on the behaviour of orthotropic steel bridge deck pavements under traffic loading. *Int. J. Pavement Eng.* 15, 471–482. doi:10.1080/10298436.2013.839790

Li, G., Cao, M., Wang, H., and Zhu, H. (2013). Stress analysis of deck pavement of continuous steel box girder. *Strategic Study CAE* 15, 79–83. doi:10.3969/j.issn.1009-1742.2013.08.014

Li, T. S., Lu, G. Y., Wang, D. W., and Hong, B. (2019). Key properties of high-performance polyurethane bounded pervious mixture. *China J. Highw. Transp.* 32, 158–169. doi:10.19721/j.cnki.1001-7372.2019.04.013

Liu G, G., Qian, Z., and Xue, Y. (2022). Comprehensive feasibility evaluation of a high-performance mixture used as the protective course of steel bridge deck pavement. *Constr. Build. Mat.* 322, 126419. doi:10.1016/j.conbuildmat.2022.126419

Liu Y, Y., Qian, Z., Gong, M., Huang, Q., and Ren, H. (2022). Interlayer residual stress analysis of steel bridge deck pavement during gussasphalt pavement paving. *Constr. Build. Mat.* 324, 126624. doi:10.1016/j.conbuildmat.2022.126624

Liu Z, Z., Zang, C., Zhang, Y., Jiang, J., Yuan, Z., Liu, G., et al. (2022). Mechanical properties and antifreeze performance of ce-ment-based composites with liquid paraffin/diatomite capsule low-temperature phase change. *Constr. Build. Mat.* 341, 127773. doi:10.1016/j.conbuildmat.2022.127773

Lu, G., Renken, L., Li, T., Wang, D., Li, H., and Oeser, M. (2019). Experimental study on the polyurethane bound pervious mixtures in the application of permeable pavements. *Constr. Build. Mat.* 202, 838–850. doi:10.1016/j.conbuildmat.2019.01.051

Lu, Z., Feng, Z.-g., Yao, D., Li, X., Jiao, X., and Zheng, K. (2021). Bonding performance between ultra-high performance concrete and asphalt pavement layer. *Constr. Build. Mat.* 312, 125375. doi:10.1016/j.conbuildmat.2021.125375

Luo, S., Lu, Q., Qian, Z., Wang, H., and Huang, Y. (2017). Laboratory investigation and numerical simulation of the rutting performance of double-layer surfacing structure for steel bridge decks. *Constr. Build. Mat.* 144, 178–187. doi:10.1016/j.conbuildmat.2017.03.172

Lv, S., Shang, T., Wang, H., and Song, Q. (2021). Research on repair Technology of existing steel-UHPC composite bridge deck. *China Concr. Cem. Prod.* 7, 88–92. doi:10.19761/j.1000-4637.2021.07.088.05

Ma, H., Zhang, Z., Ding, B., and Tu, X. (2018). Investigation on the adhesive characteristics of Engineered Cementitious Composites (ECC) to steel bridge deck. *Constr. Build. Mat.* 191, 679–691. doi:10.1016/j.conbuildmat.2018.10.056

Majumder, S., and Saha, S. (2021). Shear behaviour of RC beams strengthened using geosynthetic materials by external and internal confinement. *Structures* 32, 1665–1678. doi:10.1016/j.istruc.2021.03.107

Meng, L., Wang, Y., and Zhai, X. (2021). Experimental and numerical studies on steel-polyurethane foam-steel–concrete-steel panel un-der impact loading by a hemispherical head. *Eng. Struct.* 247, 113201. doi:10.1016/j.engstruct.2021.113201

Munoz, M. A. C., Harris, D. K., Ahlborn, T. M., and Froster, D. C. (2014). Bond performance between ultrahigh-performance concrete and normal-strength concrete. *J. Mat. Civ. Eng.* 26, 839–844. doi:10.1061/(ASCE)MT.1943-5533.0000890

Romualdi, J. P., and Mandel, J. A. (1964). Tensile strength of concrete affected by uniformly distributed and closely spaced short lengths of wire reinforcement. *J. Mat. Sci.* 61 (6), 657–672.

Shao, X. D., Huang, Z., Zhao, H., Chen, B., and Liu, M. (2013). Basic performance of the composite deck system composed of ortho-tropic steel deck and ultrathin RPC layer. *J. Bridge Eng.* 18, 417–428. doi:10.1061/(asce)be.1943-5592.0000348

Song, Y. X., Yang, J., and Wang, J. Q. (2012). Research on basic mechanical properties of polymer concrete strengthened with basalt fiber. *J. North China Inst. Water Conservancy Hydroelectr. Power* 33, 18–20. doi:10.19760/j.ncwu.zk.2012.06.005

Wang, D., Liu, P., Leng, Z., Lu, G., and Buch, M., (2017). Suitability of PoroElastic Road Surface (PERS) for urban roads in cold regions: Mechanical and functional performance assessment. *J. Clean. Prod.* 165, 1340–1350. doi:10.1016/j.jclepro.2017.07.228

Wang, H. M., Li, R. K., and Wang, X. (2014). Strength and road performance for porous polyurethane mixture. *China J. Highw. Transp.* 27, 24–31. doi:10.19721/j.cnki.1001-7372.2014.10.004

Wang, J., Dai, Q., Si, R., and Guo, S. (2019). Mechanical, durability, and microstructural properties of macro synthetic Polypropylene (PP) fiber-reinforced rubber concrete. *J. Clean. Prod.* 234, 1351–1364. doi:10.1016/j.jclepro.2019.06.272

Wang, M., Shang, F., Xiao, L., and Bao, G. (2021). Composite beam fatigue damage law of steel bridge deck gussasphalt pavement. *J. Chongqing Jiaot. Univ. Nat. Sci. Ed.* 40, 84–88+102. doi:10.3969/j.issn.1674-0696.2021.03.13

Xu, S., Xu, M., Zhang, Y., Guo, Y., Peng, G., and Xu, Y. (2020). An indoor laboratory simulation and evaluation on the aging resistance of polyether polyurethane concrete for bridge deck pavement. *Front. Mat.* 7, 237. doi:10.3389/fmats.2020.00237

Xue, Z., Wang, Y., and Wang, H. (2020). Mechanics property analysis for A new steel bridge deck pavement with UTAC-UHPC. *For. Eng.* 36, 76–84. doi:10.16270/j.cnki.slgc.2020.04.011

Yang, B., He, Z. Y., Liu, P., Li, K., Sheng, X. Y., and Li, L. (2020). Preparation and performance evaluation of polymer alloy for steel deck pavement. *Appl. Chem. Indus* 49, 3095–3102. doi:10.16581/j.cnki.issn1671-3206.20201022.003

Zeng, Z., Li, C., Wang, S., Liu, Y., Chen, Z., and Lv, Y. (2022). Study on shear performance of short bolt interface in ECC–steel bridge deck composite structure. *Appl. Sci. (Basel).* 12, 2685. doi:10.3390/app12052685

Zhang, Y., Zhang, C., Zhu, Y., Cao, J., and Shao, X. (2020b). An experimental study: Various influence factors affecting interfacial shear performance of UHPC-NSC. *Constr. Build. Mat.* 236, 117480. doi:10.1016/j.conbuildmat.2019.117480

Zhang, Y., Zhu, Y., Qu, S., Kumar, A., and Shao, X. (2020a). Improvement of flexural and tensile strength of layered-casting UHPC with aligned steel fibers. *Constr. Build. Mat.* 251, 118893. doi:10.1016/j.conbuildmat.2020.118893

Zhu, J. X., Xu, L. Y., Huang, B. T., Weng, K. F., and Dai, J. G. (2022). Recent developments in Engineered/Strain-Hardening Cementitious Composites (ECC/SHCC) with high and ultra-high strength. *Constr. Build. Mat.* 342, 127956. doi:10.1016/j.conbuildmat.2022.127956